Experimental study of Pulse Detonation Turbine Engine toward Power Generator

Takashi Sakurai[1], Tetsuro Obara[2], Shigeharu Ohyagi[2] and Motohide Murayama[3]
[1] Graduate School of Science and Engineering, Saitama University
[2] Department of Mechanical Engineering, Saitama University
255, Shimo-Okubo, Sakura-ku, Saitama, Saitama 338-8570 Japan

[3] Aero-Engine & Space Operations, IHI Co., Ltd.
229, Tonogaya, Mizuho-machi, Nishitama-gun, Tokyo 190-1297, Japan

Corresponding author, T. Sakurai: sakurai@mech.saitama-u.ac.jp

Introduction

Because of the high efficiency, the research of PDEs has been developed toward air-breathing engines[1~2)] and rockets[3)]. Recently, projects[4)] have been started applying the PDEs to turbine systems. We have planed to apply the PDE to power generator, and the performance of the systems has shown to be higher than conventional gas turbine systems by thermodynamic cycle analysis[5~6)]. In this system, problems arise at the turbine interface with the detonation wave. A detonation wave generates, a matter of course, an unsteady flow. The unsteady performance of the turbine should be estimated to predict the turbine performance. This paper describes the experimental results of Pulse Detonation Turbine Engine (PDTE). An automotive turbo-charger was attached to a PDE tube to examine its performance driven by a detonation.

Experimental

Schematic of the experimental apparatus is shown in Fig.1. A 1.12 m long, 38 mm inside diameter PDE tube was connected to the turbine inlet of turbo-charger for automobile (RHF4V, IHI) through a conjunction section (150 mm long). Hydrogen was used as a fuel and air was used as an oxidizer and a purge gas. The Shchelkin spiral was used to enhance the DDT process, and the length of the spiral was 560 mm. A type-K thermocouples (ϕ 1.6 mm) was mounted at 1.18 m from the closed end of the tube to measure the total temperature of burned gas. The outlet of the compressor was connected to a stop valve followed by an orifice flow meter to measure the mass flow rate of compressed air. A type-K thermocouples was also mounted at the outlet of compressor to measure the total temperature of compressed air.

The work done by the turbine was estimated by measuring the work done by a centrifugal compressor, assuming that there were no mechanical losses. The work done by a compressor is shown as following equation,

$$L_c = \dot{m} \cdot \left(h_{0,2} - h_{0,1}\right) = \dot{m} \cdot c_p \cdot \left(T_{0,2} - T_{0,1}\right) \qquad (1)$$

where $\dot{m}$ is the mass flow rate of compressed air, h_0 the total enthalpy, c_p the specific heat of constant pressure, T_0 the total temperature. The subscript 1 denotes the state of air at the compressor inlet and 2 denotes the state of air at the compressor outlet. The thermal efficiency was estimated by dividing this compressor work by the injected mass of fuel.

The PDTE was operated for 60 seconds in all conditions and the cycle frequency was changed at 12.5, 16 and 20 Hz. The equivalence ratio was varied from 1.56 to 2.28 by changing the reservoir pressure. The tube fill fraction was ranging from 0.80 to 1.04 and the purge fraction was ranging from 0.06 to 0.30, which were assumed at standard condition. The experimental conditions were shown in Table 1.

Results and Discussion

Figure 2 shows the total temperature of burned gas at the turbine inlet. The horizontal axis denotes elapsed time from ignition. When the PDTE started to operate, the temperature suddenly increased and took about 10 second to reach 1000 K. Then, the temperature gradually increased up to 1200 K, which showed that the PDE tube operated in quasi-stable condition. The total temperature of burned gas was much lower than the burned gas temperature of detonation, although it was considered that this temperature showed the averaged temperature of both burned gas and purge gas due to the characteristic of low responsibility of thermocouples.

Figure 3 shows the total temperature of compressed air at the compressor outlet. Before operating the PDTE, the air purge was carried out to exhaust the burned gas in previous experiment and this process caused the turbine to drive and to increase the temperature. Corresponding to the variation of turbine inlet temperature, the temperature of compressed air gradually increased. Although the temperature did not reach to the equilibrium state due to the heat loss of the system during this operation, we used the maximum temperature for estimating the thermal efficiency.

The thermal efficiency was calculated in the following procedure. For example, the experimental condition #H was used. The mass flow rate of compressed air was 0.0417 kg/s, which was obtained from the orifice flow meter. From the result of Fig.3, the total temperature of air at the compressor outlet was $T_{0,2}$=322.7 K. The total temperature of air at the compressor inlet was assumed to be equal to ambient temperature of $T_{0,1}$=298.2 K. From these values, the work done by a compressor was calculated from the equation (1);

$$L_c = \dot{m} \cdot c_p \cdot \left(T_{0,2} - T_{0,1}\right) = 1.029 \quad [\mathrm{kW}] \qquad (2)$$

where the specific heat of constant pressure c_p=1.007 kJ/kgK was used. The lower heating value (LHV) of hydrogen was $H_{H2}=1.2092\times10^5$ kJ/kg, the injected mass of hydrogen in one cycle was $m_{H2}=3.70\times10^{-5}$ kg/cycle and the cycle time at 20 Hz was 50 ms. Then, the heating value estimated by the amount of hydrogen was;

$$\dot{H}_1 = \frac{H_{H_2} \cdot m_{H_2}}{50\,ms} = 90.47 \quad [\mathrm{kW}] \qquad (3)$$

When we assumed the complete combustion of hydrogen-air, the ideal heating value was estimated as follows;

$$\dot{H}_2 = \frac{H_{H_2} \cdot m_{air}/34.3}{50\,ms} = 50.20 \quad [\mathrm{kW}] \qquad (4)$$

where the mass of air was $m_{air}=7.12\times10^{-5}$ kg/cycle and the mass ratio of stoichiometric hydrogen-air was 34.3.

Therefore, the upper and lower limit of the thermal efficiency in this condition was estimated as follows;

$$\frac{L_c}{\dot{H}_1} \le \eta_{th} \le \frac{L_c}{\dot{H}_2} \quad (5)$$

$$1.14\times10^{-2} \le \eta_{th} \le 2.05\times10^{-2}$$

The results of each condition are summarized in Table 2. Thermal efficiency obtained in this experiment was much lower than the thermal efficiency predicted by the thermodynamic cycle analysis. This is primarily attributed to the discrepancy of the mass flow between the PDTE and the turbo-charger, and it is secondly considered that the turbo-charger used in this research was not suitable for the PDTE because of its flow characteristic.

Figure 4 shows the turbine inlet temperature, which is an important parameter for evaluating the turbine performance. The temperature increased as the cycle frequency increased. Since the cycle frequency means the repetition rate of combustion, this is easily understood. The dependency of the thermal efficiency on the equivalence ratio is shown in Fig.5. In contrary to the theoretical prediction, the thermal efficiency showed the best performance in fuel-rich condition ranging from 1.8 to 2.0. This discrepancy was attributed to the uniformity of the fuel. The turbine inlet temperature related to the work done by compressor, hence the thermal efficiency resulted in better performance at 20 Hz than 12.5 Hz.

Concluding Remarks

An experimental study of the PDTE, which is comprised from an automotive turbo-charger attached to a PDE tube, was carried out to examine its performance. The estimated thermal efficiency was lower than that predicted by thermodynamic cycle analysis. This is because the discrepancy of mass flow between the PDTE and the turbo-charger. In addition, due to the pulse flow of PDTE, the suitable turbine must be considered to extract power from detonation efficiently. In this PDTE, the thermal efficiency showed better performance in fuel-rich condition. This is attributed to the uniformity of the mixture, so that we have to improve the injection assembly for better mixing. As a first step, we demonstrated that it is possible to extract power from PDE by the turbine system.

References

1) Hoke, J., Bradley, R., Stutrud, J. and Schauer, F.: Integration of a Pulsed Detonation Engine with an Ejector Pump and with a Turbo-charger as Methods to Self-Aspirate, AIAA 2002-0615.
2) Schauer, F., Bradley, R. and Hoke, J.: Interaction of a Pulsed Detonation Engine with a Turbine, AIAA 2003-0891.
3) Kasahara, J., Hirano, M., Matsuo, A., Sato, S., Endo, T. and Satori, S.: Flight Experiments Regarding Ethylene-Oxygen Single-Tube Pulse Detonation Rockets, AIAA 2004-3918.
4) Rasheed, A., Tangirala, V.E., Vandervort, C.L., Dean, A.J.and Haubert, C.: Interactions of a Pulsed Detonation Engine with a 2D Turbine Blade Cascade, AIAA 2004-1207.
5) Murayama, M., Obara, T. and Ohyagi, S.: Feasibility Study on Pulse Detonation Engine for Power Generator, Symposium on Shock Waves in Japan, 2003, pp.365-366 (in Japanese).
6) Sakurai, T., Yamane, N., Obara, T., Ohyagi, S., and Murayama, M.: A Study on Thermodynamic Cycle of Pulse Detonation Gas Turbine Engine, ISABE-2005-1047 (2005).
7) Heiser, W.H. and Pratt, D.T.: Thermodynamic Cycle Analysis of Pulse Detonation Engines, *J. Propulsion Power*, **18** (2002), pp.68-76.

8) Wintenberger, E. and Shepherd, J.E.: Thermodynamic Analysis of Combustion Processes for Propulsion Systems, AIAA 2004-1033.
9) Endo, T., Kasahara, J., Matsuo, A., Inaba, K., Sato, S. and Fujiwara, T.: Pressure History at the Thrust Wall of a Simplified Pulse Detonation Engine, *AIAA J.*, **42** (2004), pp.1921-1930.
10) Sakurai, T., Minagawa, T., Yoshihashi, T., Obara, T., and Ohyagi, S.:A Study for Development of Hydrogen-fueled Pulse Detonation Engines, Sci. Tech. Energetic Materials, **65** (2004), pp.125-133.
11) Sakurai, T., Ooko, A., Yoshihashi, T., Obara, T., and Ohyagi, S.: Investigation of the Purge Process on the Multi-cycle Operations of a Pulse Detonation Engine, *Trans. Jpn. Soc. Aeronaut. Space Sci.*, (2005), Accepted.

Table 1 Experimental conditions

#	Hz	Time [s]	Cycle	ER	FF*	PF*
A	12.5	60	750	1.56	0.90	0.30
B	↓	↓	↓	1.82	0.94	0.29
C	↓	↓	↓	2.28	0.98	0.28
D	16	↓	480	1.59	0.82	0.24
E	↓	↓	↓	1.71	0.90	0.24
F	↓	↓	↓	1.92	1.04	0.26
G	20	↓	1200	1.62	0.80	0.06
H	↓	↓	↓	1.80	0.84	0.17
I	↓	↓	↓	2.04	0.88	0.17

* calculated at standard condition

Table 2 Results of each condition

	A	B	C	D	E	F	G	H	I
Frequency [Hz]	12.5	→	→	16	→	→	20	→	→
FF	0.90	0.94	0.98	0.82	0.90	1.04	0.80	0.84	0.88
ER	1.56	1.82	2.28	1.59	1.71	1.92	1.62	1.80	2.04
TIT [K]	816.0	1046.5	1009.7	927.1	1126.5	1128.6	1133.4	1200.8	1210.0
Temp. at compressor	9.20	15.87	13.14	11.18	15.08	23.17	17.91	24.51	26.14
Mass flow rate [kg/s]	0.0239	0.0318	0.0293	0.0286	0.0330	0.0385	0.0344	0.0417	0.0426
Mass flow rate [m3/min]	1.112	1.480	1.364	1.328	1.534	1.792	1.600	1.940	1.981
Compressor work [kW]	0.221	0.509	0.388	0.321	0.501	0.898	0.620	1.029	1.121
Mass of H2 [g/cycle]	0.037	0.042	0.050	0.034	0.039	0.048	0.034	0.037	0.042
Mass of air [g/cycle]	0.816	0.797	0.751	0.736	0.789	0.857	0.717	0.712	0.706
Heat release (1) [kW]	55.90	63.79	75.62	65.88	75.97	93.01	81.79	90.47	101.46
Heat release (2) [kW]	33.94	35.11	33.10	41.52	44.51	78.35	50.53	50.20	49.80
Thermal efficiency [%]	0.40-0.61	0.80-1.45	0.51-1.17	0.49-0.77	0.66-1.13	0.97-1.86	0.76-1.23	1.14-2.05	1.10-2.25

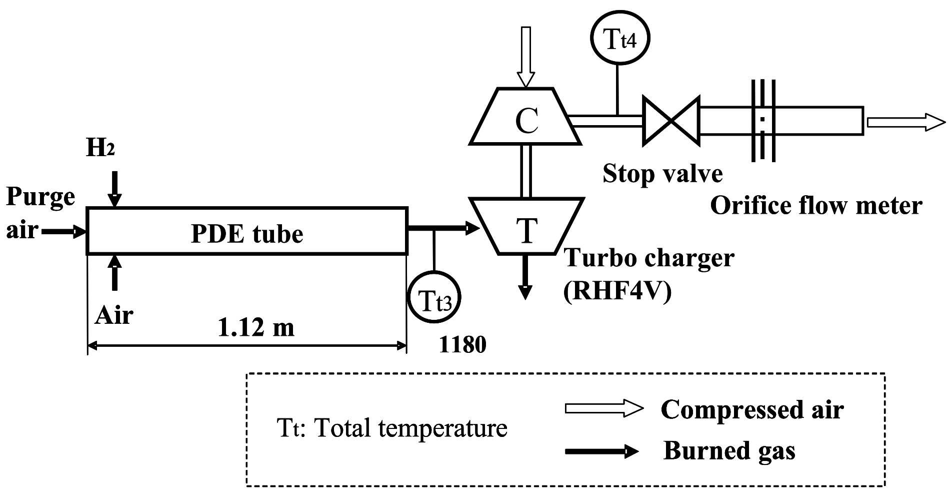

Fig.1 Schematic of experimental apparatus

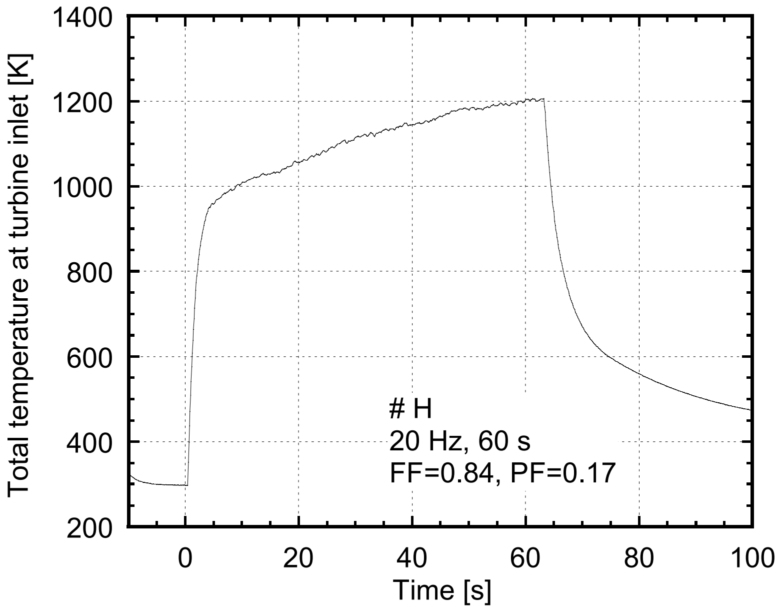

Fig.2 Total temperature at turbine inlet at 20Hz, 60s operation

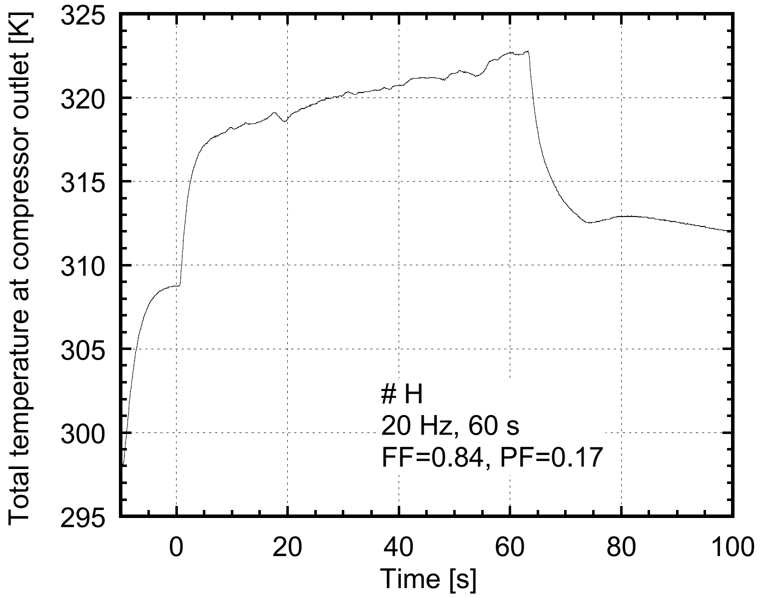

Fig.3 Total temperature at compressor outlet at 20 Hz, 60 s operation

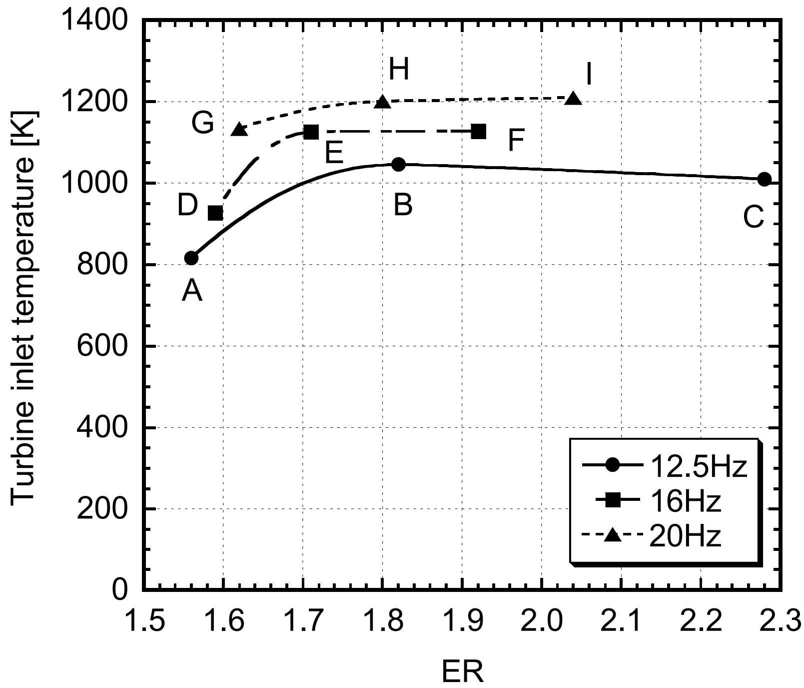

Fig.4 Turbine inlet temperature of each condition

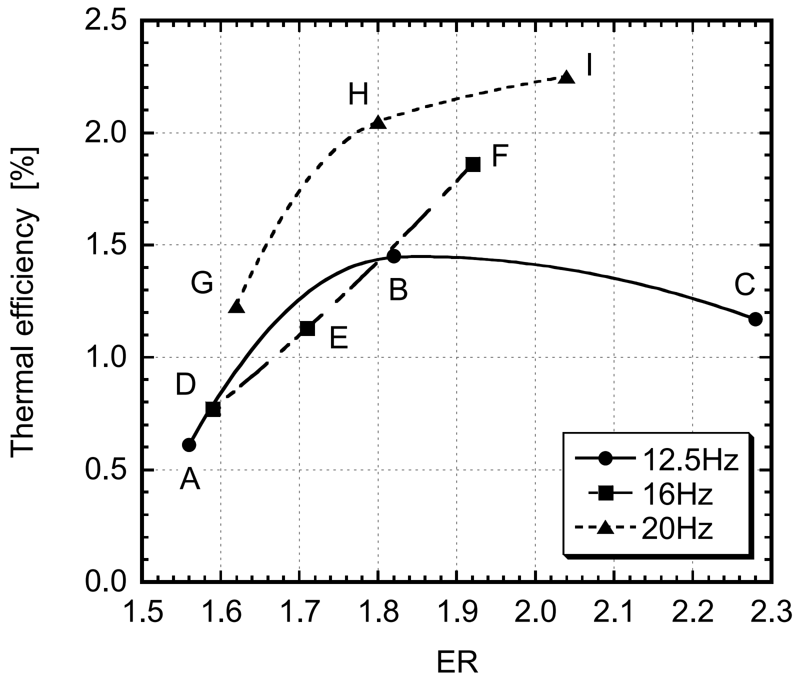

Fig.5 The dependency of the thermal efficiency on equivalence ratio